Atmósfera (2000) 13, pp. 147-166

Sensitivity of Asian summer monsoon and tropical circulations to 1987 and 1988 sea surface temperature anomalies

BIJU THOMAS

CNRM/GMME, 42, Av. G. Coriolis, 31057 Toulouse Cedex, France

S. V. KASTURE

Physical Research Laboratory, Ahmedabad - 380009, India

V. SATYAN

Indian Institute of Tropical Meteorology, Pune - 411008, India

(Manuscript received Sept. 3, 1998; accepted in final form Sept. 24, 1999)

RESUMEN

En este trabajo el impacto de las temperaturas de superficie del mar (SST's) durante 1987 y 1988 sobre el monzón medio estibal del Hemisferio Norte se estudia usando un modelo atmosférico de circulación general. Cuatro experimentos se hicieron para comprobar las relaciones entre los impactos de campos de SST en las regiones oceánicas global (E_1), tropical (E_2), Pacífico tropical (E_3) y tropical central y oriente (E_4).

Se vio que en E_1, el modelo capturaba ciertos rasgos de importantes circulaciones y precipitaciones de los monzones de 1987 y 1988. El exflujo troposférico superior en 1988 fue intenso sobre La India, el océano Indico y la Australia occidental y el influjo fue, asimismo, intenso sobre las regiones central y oriente del océano Pacífico. Durante 1987 el mínimo del potencial de velocidad de la troposfera superior sobre el Pacífico occidental cambió 20°hacia el este de su posición en 1988.

El chorro tropical del este (TEJ) sobre el Africa equatorial fue más intenso en 1988 que en 1987. El máximo de lluvia sobre el Pacífico occidental cambió hacia el Pacífico central y del este durante 1987. Sobre La India meridional, el océano Indico suroccidental y El Sahel, hubo un incremento en la lluvia en 1988 en comparación con la de 1987. Sin embargo, ésta fue menor sobre la India nororiental en 1988 que en 1987.

En los experimentos e_2, E_3 y E_4 la diferencia en las estructuras de gran escala en el potencial de velocidad de la troposfera superior entre 1987 y 1988 fueron semejantes a los de E_1. No obstante, algunos cambios importantes se vieron en E_3 y E_4. El flujo divergente en 1988 fue más sobre el océano Indico y la región monzónica con el centro de las diferencias en el potencial de velocidad cambiando más hacia el este en E_3 y E_4 que en E_1. Cambios congruentes se observaron también en los campos eólicos. El chorro tropical del este durante ambos años de 1987 y 1988 fue más débil en E_3 y E_4 que E_1.

ABSTRACT

In this work, the impact of Sea Surface Temperatures (SSTs) during 1987 and 1988 on the Northern Hemisphere summer mean monsoon is studied using an Atmospheric General Circulation Model. Four model experiments were carried out to assess the relative impacts of observed SST fields of global(E1), tropical(E2), tropical Pacific(E3) and tropical central and eastern Pacific(E4) oceans. It was seen that in E1, the model captured a number of important observed circulation and precipitation features of 1987 and 1988 monsoons. The upper tropospheric outflow during 1988 was strong over India, Indian ocean and western Australia and the inflow was strong over central and eastern Pacific oceans. During 1987, the upper tropospheric velocity potential minimum over western Pacific shifted east by 20^o of its 1988 position. The Tropical Easterly Jet (TEJ) over equatorial Africa was stronger in 1988 than in 1987. The precipitation maximum over western Pacific shifted to central and eastern Pacific during 1987. Over southern India, south west Indian ocean and parts of Sahel, there was increased rainfall during 1988 compared to 1987. However, it was less over northeast India in 1988 than in 1987.

In experiments E2, E3 and E4, the large-scale structures of the upper tropospheric velocity potential difference between 1987 and 1988 were similar to those in E1. However, some important changes were seen in E3 and E4. The divergent flow during 1988 was weaker over Indian ocean and monsoon region with the center of velocity potential differences shifted to the east in E3 and E4 than in E1. Consistent changes were seen in the wind fields also. The TEJ was weaker during both the years 1987 and 1988 in E3 and E4 than in E1.

1. Introduction

Tropical and monsoon circulations exhibited remarkable interannual variability during 1987 and 1988. During 1987, a severe drought occurred in Sahel and the June-August (JJA) rainfall over India was less than its long-term average. On the other hand, during 1988 summer, Sahel region experienced normal rainfall and Indian rainfall was above normal. At the same time, the sea surface temperature anomalies (SSTA) over tropical Pacific underwent dramatic changes during 1987 and 1988 in connection with warm (El Niño) and cold (La Niña) phases of El Niño and Southern Oscillations (ENSO) cycle (Fig. 1). Recent studies have shown that ENSO affect global climate in such a way that a section of globe experiences drought while other sections experience excessive rainfall, and its impacts last for as long as 24 months. The Tropical Ocean and Global Atmosphere program (TOGA) has focussed on the seasonal time scale prediction of climate using Coupled Ocean Atmospheric General Circulation Models (CGCMs). This requires that the atmospheric part of a CGCM produces reasonable simulation of circulation anomalies when it is forced by SSTA. Keeping this in mind, many modeling groups integrated their AGCMs with the SSTA of 1987 and 1988. If the two-dimensional SSTA can produce deep three-dimensional heating anomalies in the atmosphere, then it can change the large-scale circulations (Shukla, 1986). In an AGCM, the relationship among SSTA, diabatic heating anomalies and circulation anomalies mainly depends on the physical parameterizations incorporated in it. However, AGCMs differ in their parameterizations of various physical processes and in their horizontal and vertical resolutions. Thus, there is a need to assess the response of each AGCM to observed SSTA.

Palmer *et al.* (1992) carried out a number of AGCM sensitivity experiments with SSTA at different locations, that occurred during 1987 and 1988, and with different initial conditions. They concluded that the European Center for Medium-Range Weather Forecasting (ECMWF) AGCM has reasonable skill to simulate the observed variability in the global-scale velocity potential and stream function fields when it is forced by observed SSTA. They also noted that the ECMWF model simulated velocity potential and stream function anomalies are insensitive to the initial conditions, and the SSTA over Pacific have the largest influence on the tropical large-scale flow in comparison with Indian and Atlantic Ocean SSTA. The observational study of Shukla and Paolino (1983) suggested that Indian monsoon rainfall is correlated more strongly with Pacific SST than Indian Ocean SST. Zhu and Houghton (1996) imposed idealized SSTA over Indian Ocean in the National Center for Atmospheric Research (NCAR) Community Climate model

1 (CCM1) and found that the large-scale hydrological cycle and circulation components serve as internal feedback mechanisms influencing the response of the Asian summer monsoon to the external forcing exerted by SSTA in the Indian Ocean. Some of the other modeling efforts to simulate the circulation anomalies of 1987 and 1988 include Mo (1992), Druyan and Hastenrath (1994) and Laval *et al.* (1996). Using NCAR CCM1, Chen and Yen (1994) demonstrated that interannual variability of steady tropical heating at eastern Pacific induced by interannual variation of eastern Pacific SSTA results in the interannual variation of summertime stationary eddies and associated Asian monsoon since Asian monsoon is a part of summertime stationary eddies. On the other hand, from observational analysis, Barnett *et al.* (1989) found that the changes in the eastern Pacific SSTA are coincident with summer monsoon rainfall or eastern Pacific SSTA are lagging the Asian monsoon.

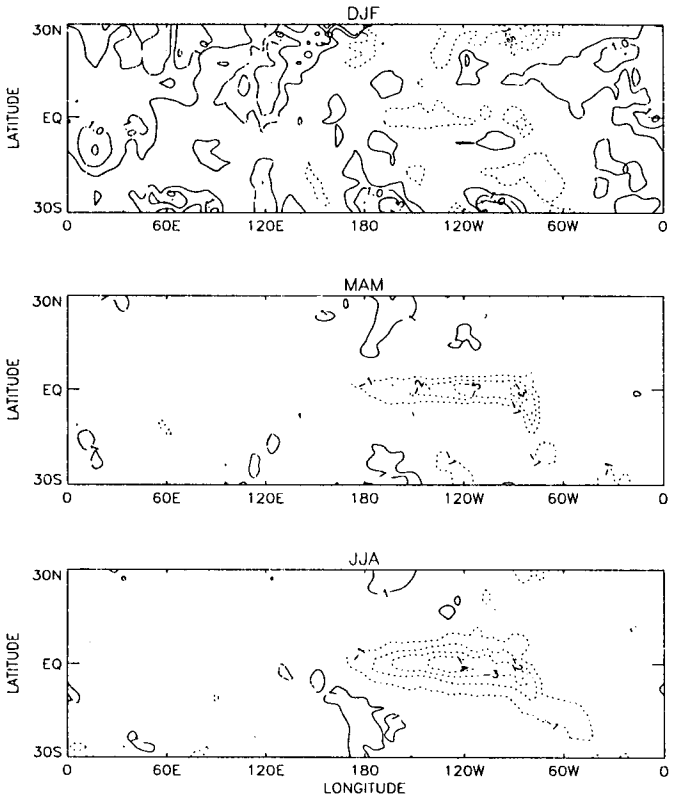

Fig. 1. SST (^{o}C) difference between 1988 and 1987 for DJF (1a), MAM (1b) and JJA (1c). Isopleth spacing is .5^{o}C for DJF and 1^{o}C for MAM and JJA. Broken lines indicate negative values.

The studies of Sud and Smith (1985), Barnett *et al.* (1989), Vernekar *et al.* (1995) and Meehl (1994) emphasized the importance of land-surface processes over Asian continent for the interannual variation of Asian monsoon. Using UK Universities' Global Atmospheric Modeling Programme (UGAMP) AGCM and ECMWF analysis, Ju and Slingo (1995) linked the strength of broad-scale Asian summer monsoon to the latitudinal position of Intertropical Convergence Zone (ITCZ) over Indonesia and western Pacific. The UGAMP AGCM outputs did not show any relationship between Eurasian winter snow cover (EWSC) and the following Asian summer monsoon. In a recent observational study, Yang (1996) demonstrated that ENSO plays a more important role than EWSC in influencing the interannual variation of Asian summer monsoon.

His study suggests that the usual inverse EWSC-monsoon relationship is disrupted during El Niño period. In essence, these studies indicate that the key factors, that determine the interannual variability of Asian monsoon, are the slowly varying surface boundary conditions (both remote and regional) like SSTs, the land-surface processes over the continent and the complex interactions between these two.

From the above discussions, it is clear that there is a need to find the influence of each of these components on the variability of Asian monsoon using many AGCMs. It is difficult to assess the individual role of SSTs and land-surface processes on the interannual variability of Asian summer monsoon from some of the above studies like Palmer *et al.* (1992), Mo (1992) and Druyan and Hastenrath (1994). Additionally, results of these studies are the response of AGCMs to JJA SSTA only. However, the strength of Asian summer monsoon may be influenced by the previous spring SSTA over subtropical north-west Pacific (Ju and Slingo, 1995). If the surface boundary conditions like SSTs strongly influence the year to year variability of Asian monsoon and these surface boundary conditions are predictable, then the dynamical prediction of the year to year variability of monthly or seasonal average monsoon circulation is possible. Since the SSTA over tropical Pacific associated with 1992 El Niño was successfully predicted and land-surface processes over Asian continent are non-linear, it will be interesting to know to what extent an AGCM can simulate observed interannual variability of circulations when among many surface boundary conditions only SSTs have interannual variations. And if it can simulate the circulation anomalies reasonably well, then it will be interesting to know the individual role of tropical SSTA, tropical Pacific SSTA and tropical central and eastern Pacific SSTA on the large-scale east-west and north-south monsoonal circulations.

With this background we present the results of four integrations with our AGCM in the following sections. In section 2, we describe the model and the experiments. In the section 3, we present the results of first integration and section 4 contains results of second, third and fourth integrations. Discussions and conclusions are included in section 5.

2. The model and the experiments

The AGCM used in this study is the general circulation model described in Biju Thomas *et al.* (2000). This model is a global spectral AGCM truncated at rhomboidal wavenumber 21 and has six vertical levels. The model has smooth orography, planetary boundary layer, deep convection (modified Kuo's scheme), large-scale condensation, radiation with interactive clouds and diurnal cycle.

In the first experiment (E1), the AGCM was integrated for eight months from January 1^{st} with observed monthly mean SSTs of 1987 and 1988. Three more separate experiments (E2, E3 and E4) were designed for eight months from January 1^{st}. In E2 and E3, the model was integrated with observed SSTs of 1987 and 1988 over tropical region and tropical Pacific region respectively and other oceanic regions were masked by climatological SSTs. In the fourth experiment (E4), AGCM integration was performed with climatological SSTs in all oceanic grid points except tropical central and eastern Pacific where observed monthly mean SSTs of 1987 and 1988 were used. Table 1 illustrates the regions where the observed monthly mean SSTs are used. An eight months control simulation was also performed by forcing the model with climatological SSTs over all oceans (EC). All the integrations described above were performed with monthly mean SSTs from January to August. During the course of model integration, to allow a smooth transition between monthly values, the SST values were updated daily by interpolating from the adjacent months.

Table 1:

Integration	Sea surface temperature
E1	Observed Global SST
E2	Observed SST over (0°-360° , 30°S-30°N) Climatological SST elsewhere
E3	Observed SST over (110°E-100°W , 30°S-30°N) Climatological SST elsewhere
E4	Observed SST over (170°E-100°W , 30°S-30°N) Climatologcal SST elsewhere

The initial conditions for all these four experiments were taken from the six year simulation by the same AGCM as described in Biju Thomas *et al.* (2000). The justification for not using observed initial conditions is based upon the finding of Palmer *et al.* (1992) that the simulated large-scale seasonal mean velocity potential and stream function fields in the tropics are relatively insensitive to the atmospheric initial conditions as compared to the boundary conditions like SSTs. A recent study by Shukla and Fennessy (1994) has also shown that the simulated rainfall anomalies during 1987 and 1988 do not have much sensitivity to the initial conditions. In all our four experiments, among many surface boundary conditions, only SSTs were having interannual variations.

For comparison with observations, we have used NCEP/NCAR (National Center for Environmental Prediction/National Center for Atmospheric Research) reanalysis for winds, velocity potential and precipitation. Hereafter NCEP/NCAR reanalysis will be referred as analysis or observations. The OLR is taken from NOAA POLAR ORBITER OLR data sets. The monthly mean observed and climatological SSTs were derived from Reynolds and Marsico (1993).

3. Results of Experiment 1

3.1 Velocity potential

Since the divergent flow in tropics is largely directly driven by diabatic heating, the velocity potential field will give an idea of three-dimensional heating anomalies associated with SSTA. The simulated JJA mean velocity potential fields for 1987 and 1988 are displayed in Figures 2a and 2b respectively. Figure 2c shows the JJA mean velocity potential difference between 1988 and 1987. Figures 3a, 3b and 3c are corresponding observed counterparts from reanalysis datasets analyzed in the model resolution. The detailed evolution of the observed planetary scale upper level divergent circulations for 1987 and 1988 is well documented in Krishnamurti *et al.* (1989, 1990).

The simulated velocity potential field shows wave number one structure with divergent outflow over India and western Pacific and divergent inflow over eastern Pacific, Atlantic and American and African continents. During 1988, the divergent outflow center has a westward shift compared to 1987 associated with the migration of heat source over tropical Pacific. In 1988, divergent flow becomes strong over Indian ocean compared to 1987. It can be seen by comparing with observations that all these modeled features are quite realistic. The model has captured the intensification of Walker cell associated with 1988 La Niña with ascending motion over western Pacific and descending motion over eastern Pacific. The width of the Walker cell during 1987

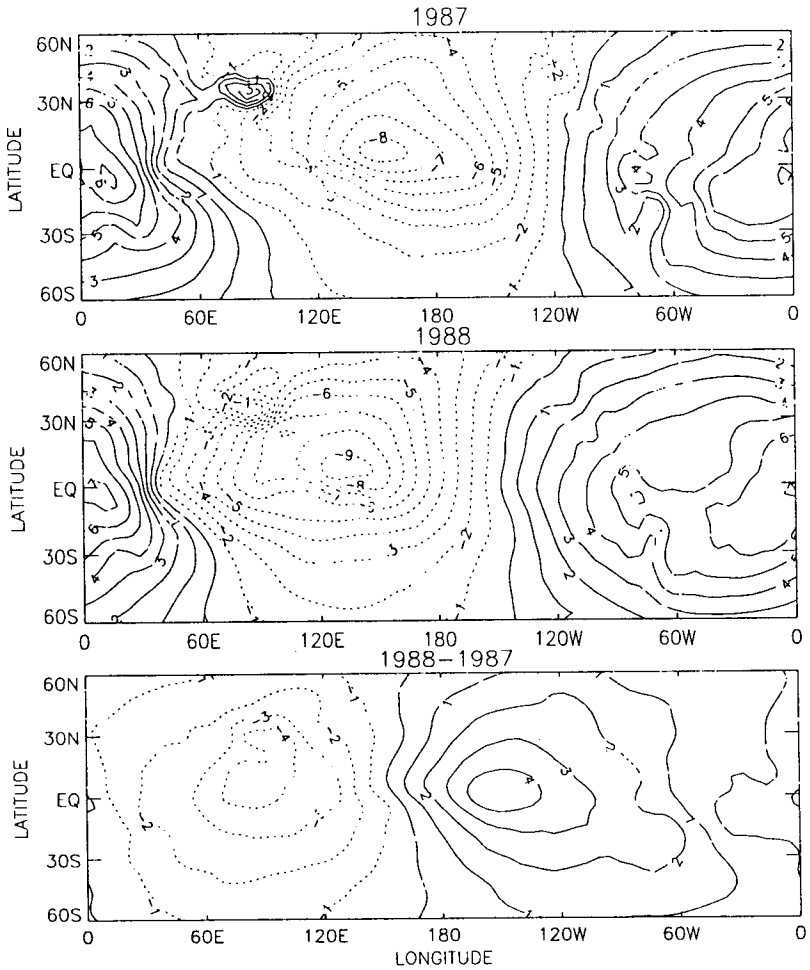

Fig. 2. Modeled JJA Velocity potential for 1987 (2a), 1988 (2b) and 1988 minus 1987 (2c) respectively. Contour interval is $1\times10^{6}m^{2}s^{-1}$. Broken lines indicate negative values.

and 1988 has reasonable agreement with observations. However, the model simulated velocity potential is weaker in both 1987 and 1988 compared to the analyzed velocity potentials. It is worthwhile to note here that there are considerable differences between NCEP/NCAR reanalyzed and ECMWF analyzed velocity potential. The ECMWF analyzed velocity potential field during 1987 has maximum negative contour -12 over western Pacific and maximum positive contour 10 over south Africa (Fig. 2 of Druyan and Hastenrath, 1994). Corresponding contour values of ECMWF analyzed velocity potential field for the year 1988 are -14 and 12 respectively. The NCEP/NCAR reanalysis shows much larger contour values (Figs. 3a and 3b) than those in ECMWF analysis. The simulated velocity potential fields have small scale features around 30°N, which appear to be related to the orographic effect over Himalayas. Similar discrepancies are found in similar experiments with the Goddard Institute for Space Studies (GISS) GCM (Druyan and Hastenrath, 1994) and Australian Bureau of Meteorological Research Center (BMRC) GCM (Frederiksen *et al.*, 1992).

The modeled JJA mean velocity potential difference (1988 minus 1987) has a dipole structure with negative center over African and Asian continents and positive center over central and eastern Pacific in connection with stronger upper level divergence over Indian Ocean and Asian continents and stronger upper level convergence over central and eastern Pacific. The position

of maximum positive center over central and eastern Pacific matches well with observations. However, the position of maximum negative center over Indian subcontinent is slightly shifted eastwards compared to observations. The positive center appearing in the NCEP/NCAR analysis is stronger than modeled field. Again, the ECMWF analysis (Fig. E2, World Meteorological Organization, 1992) exhibits a weaker positive center over central and eastern Pacific compared to NCEP/NCAR reanalysis and the split of two maximum centers over central and eastern Pacific is not seen in the ECMWF analysis as in our model simulation. Overall, the simulated velocity potential difference is closer to ECMWF analysis than NCEP/NCAR reanalysis.

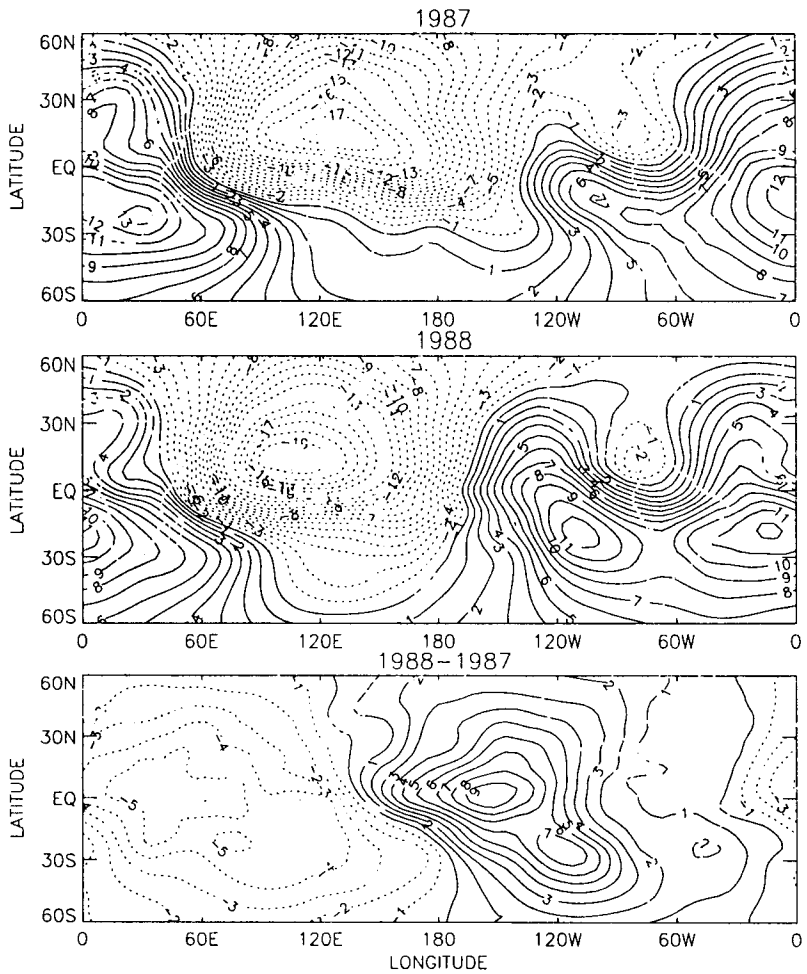

Fig. 3. Same as Figure 2 except for observations.

3.2 Horizontal wind

The model simulated 200mb JJA mean winds for 1987, 1988 and difference between 1988 and 1987 are presented in Figures 4a, 4b and 4c respectively. Figures 5a, 5b and 5c are corresponding fields from observations. The simulated winds for the years 1987 and 1988 show the main features like strong easterlies over tropical Africa, Arabian sea, Indian Ocean and southern part of India, weak easterlies over tropical Pacific and subtropical westerlies. We note that AGCM captures the correct amplitude of the wind speed at the core of TEJ during both 1987 and 1988. Chen

and Loon (1987) showed from observational analysis that the TEJ is generally weaker during the summer warm phase of ENSO when positive SSTA appear over central and eastern Pacific. The weakening of TEJ over tropical Africa, Indian Ocean, Arabian sea and southern part of India is well reproduced by the model during the El Niño year 1987. Thus our model has properly responded to the warm SSTA over central and eastern Pacific associated with 1987 El Niño. Another two observed features during 1988, which are well simulated by the model, include the southward extension of easterlies over 0 - 100°E and weak easterlies over tropical Pacific. However, during 1987, the simulated easterlies are weaker than observations especially over east of dateline. The strengthening of easterlies over Central America and Central Atlantic is seen both in observations and simulations during 1988. The easterlies over Atlantic have lesser zonal westward extension into Central America during 1987 compared to 1988. The south Asian anticyclone is simulated at correct latitude (20-30°N), but it has a westward shift compared to observations.

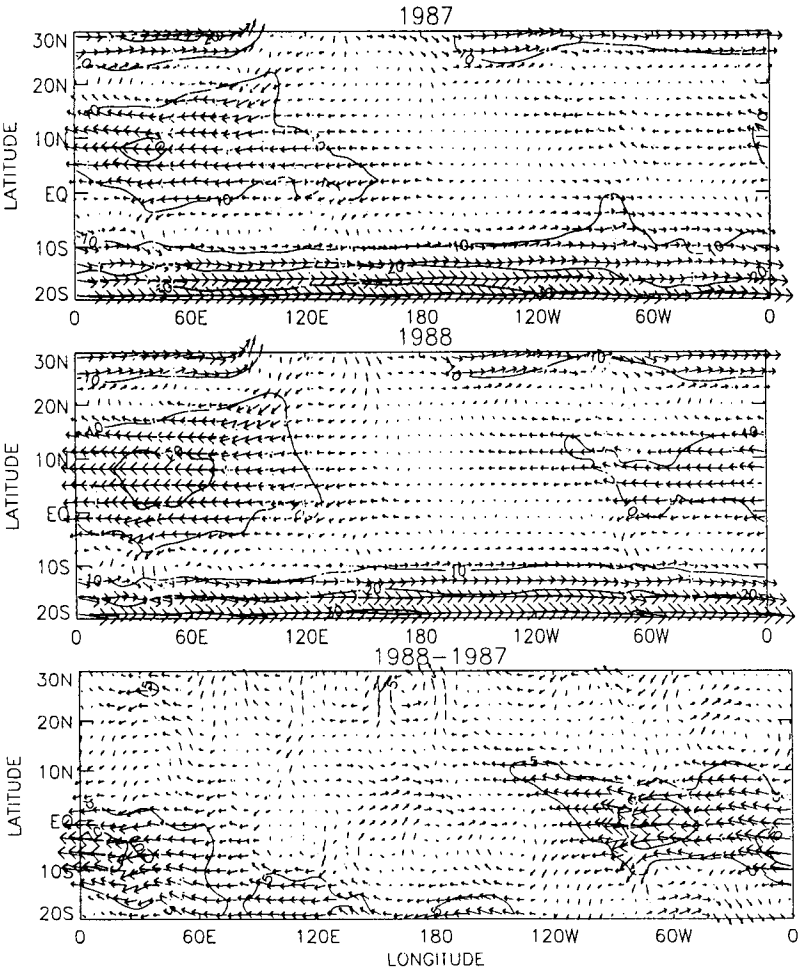

Fig. 4. Modeled JJA wind for 1987 (4a), 1988 (4b) and 1988 minus 1987 (4c) respectively. Contours of wind speed are overplotted with contour interval 10 ms^{-1} for Figures 4a and 4b and 5 ms^{-1} for Figure 4c.

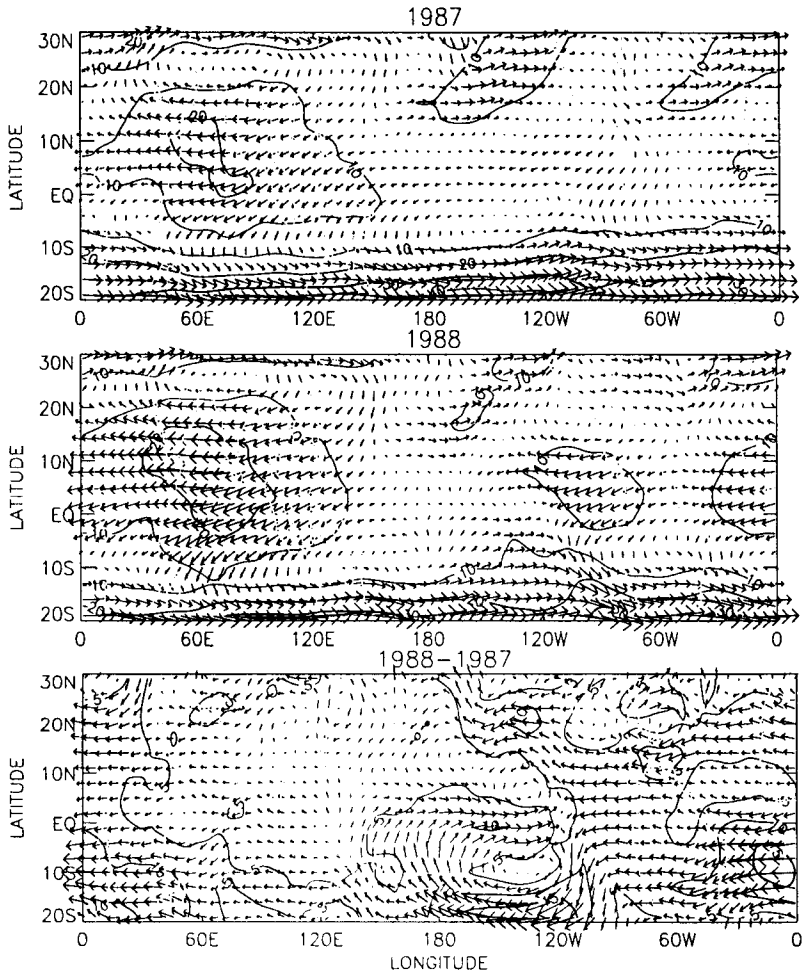

Fig. 5. Same as Figure 4 except for observations.

The difference of simulated winds between 1988 and 1987 shows stronger TEJ over northern Africa, Indian Ocean, Arabian sea and south part of India during 1988. However, the amplitude of the difference of the simulated winds over northern Africa is lesser than that of the observed winds. It can be seen that the AGCM successfully simulates the weakening of westerlies over south of Africa near 15°S. The analysis shows westerly wind differences (1988 minus 1987) over central Pacific in between 140°E and 120°W. The model captures this westerly wind differences with lesser amplitude and lesser zonal width. Over Central America, the model simulates stronger easterly wind differences like in observations. Overall, we note that AGCM does a better job in capturing most of the observed features of the circulation anomalies that occurred during 1987 and 1988.

3.3 Precipitation rate

Following Gadgil *et al.* (1992) and Gadgil and Raju (1995), there are four preferred heavy rainfall zones over Indian longitudes. They are (1) the rain belt associated with ITCZ around 20°N stretching across the continent from Bay of Bengal (Gadgil and Raju, 1995, call this region as monsoon convergence zone (MCZ)) (2) heavy rainfall during JJA over Himalayan region forced by the mountains (3) rainfall over western Ghats on the west coast of Peninsular India (4) the

ITCZ over the equatorial warm Indian Ocean between 0 - 10°S across the Indian longitudes. The observed July mean OLR distribution, analyzed at 2.5×2.5 resolution, is shown in Figure 6. The OLR field depicts the four zones of OLR minima, which indicate the presence of cooler cloud tops associated with deep convection and rainfall during Indian summer monsoon. The Figure 7 exhibits the distributions of mean JJA precipitation simulated by the AGCM when it is integrated with climatological SSTs. In this climatological SST run (EC), the duration of integration and initial conditions are same as in E1. An intense rainfall pattern over Himalayan region and a rainfall maximum over western Ghats are seen in the climatological SST run. The mean July OLR field (Fig. 6) shows a minimum over west coast of Burma which implies strong convective activity over this region. A well defined strong rainfall maxima can be seen over the west coast of Burma in the climatological SST run (Fig. 7). However, the rainfall maxima at MCZ and Indian Ocean are poorly simulated in this run. The simulated JJA mean rainfall over western Pacific has good agreement with the seasonal precipitation climatology of Legates and Wilmott (1990).

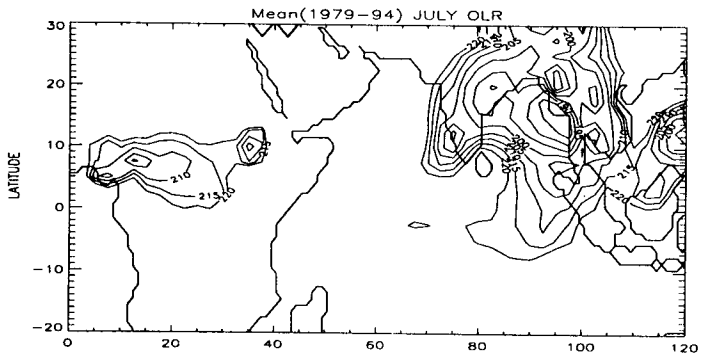

Fig. 6. July mean NOAA polar orbitter OLR(Wm^{-2}) data averaged during the period 1979 to 1994. Plotted contours are 160, 165, 170, ..., 215, 220 Wm^{-2}.

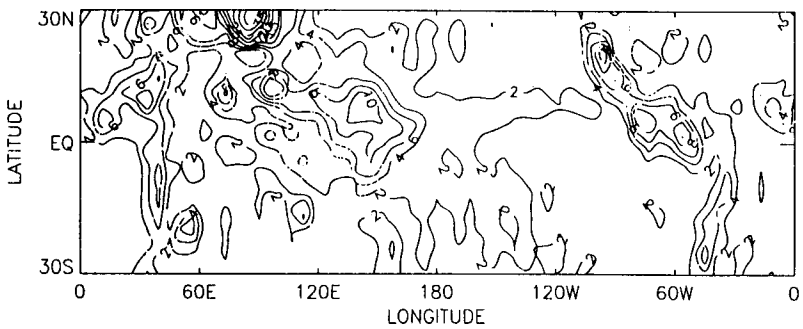

Fig. 7. June-August precipitation rate (mm day^{-1}) from climatological SST run. Plotted contours are 2, 4, 6, 8, 10, 15, 20, .. mm day^{-1}.

The distributions of simulated JJA mean precipitation rate for 1987, 1988 and 1988 minus 1987 are shown in Figures 8a, 8b and 8c respectively. Corresponding observed fields are shown in Figures 9a, 9b and 9c respectively. The observed rainfall field shows an intense precipitation band from 2°S to 14°N over Africa during 1987 and 1988 (Figs. 9a and 9b). This rain band is associated with ITCZ over tropical Africa. This feature is well reproduced by the model (Figs. 8a and 8b). A narrow tongue of precipitation pattern can be seen over east coast of southern part of Africa in the model simulations. This pattern appears to be related to the orography there and it is not seen in the analysis especially during 1988. It is interesting to note that the

CAMS/MSU proxy (Fennessy, 1993) shows a pattern similar to our model simulation. During both 1987 and 1988, the model has captured the heavy rainfall over Himalayas and the rain belt over Indian Ocean associated with the oceanic part of ITCZ and a weak rainfall maximum over west coast of Peninsular India. However, AGCM simulates too weak MCZ around 20°N. We have noted a similar deficiency in the climatological SST run also (Fig. 7). The ITCZ across Central America is well simulated by the model for 1987 and 1988 (Figures 8a, 8b and 9a, 9b). Also, both simulations and observations (Figures 8a, 8b and 9a, 9b) show the northward extension of rainfall pattern over American continent.

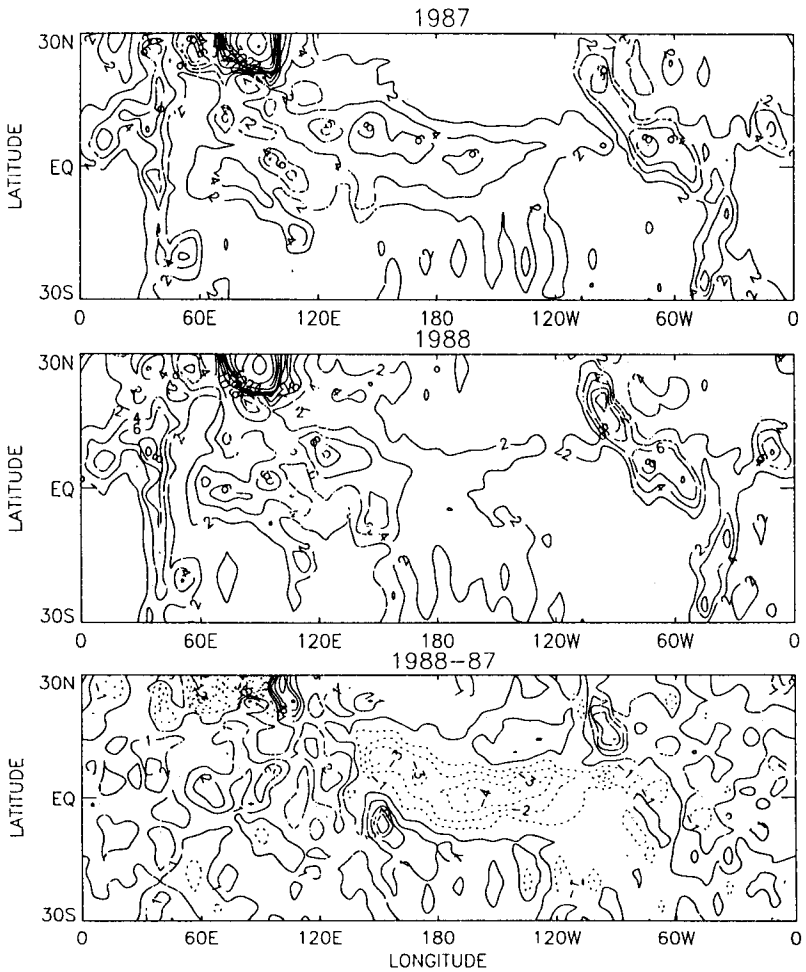

Fig. 8. Modeled JJA precipitation rate (mm day^{-1}) for 1987 (8a), 1988 (8b) and 1988 minus 1987 (8c) respectively. Plotted contours are 2, 4, 6, 8, 10, 15, 20,.. mm day^{-1} for Figures 8a and 8b. Contour interval is 1 mm day^{-1} for Figure 8c. Zero contour is suppressed. Broken lines indicate negative values.

One of the dominant features in the simulated rainfall differences (1988 minus 1987) is the largest negative rainfall differences over equatorial central and eastern Pacific. Trenberth (1976) noted that during ENSO year, ITCZ and SPCZ (Southern Pacific Convergence Zone) have southward and north-eastward shift respectively and, as a result, the two convergence zones come close together in the western Pacific. The positive precipitation anomalies over south

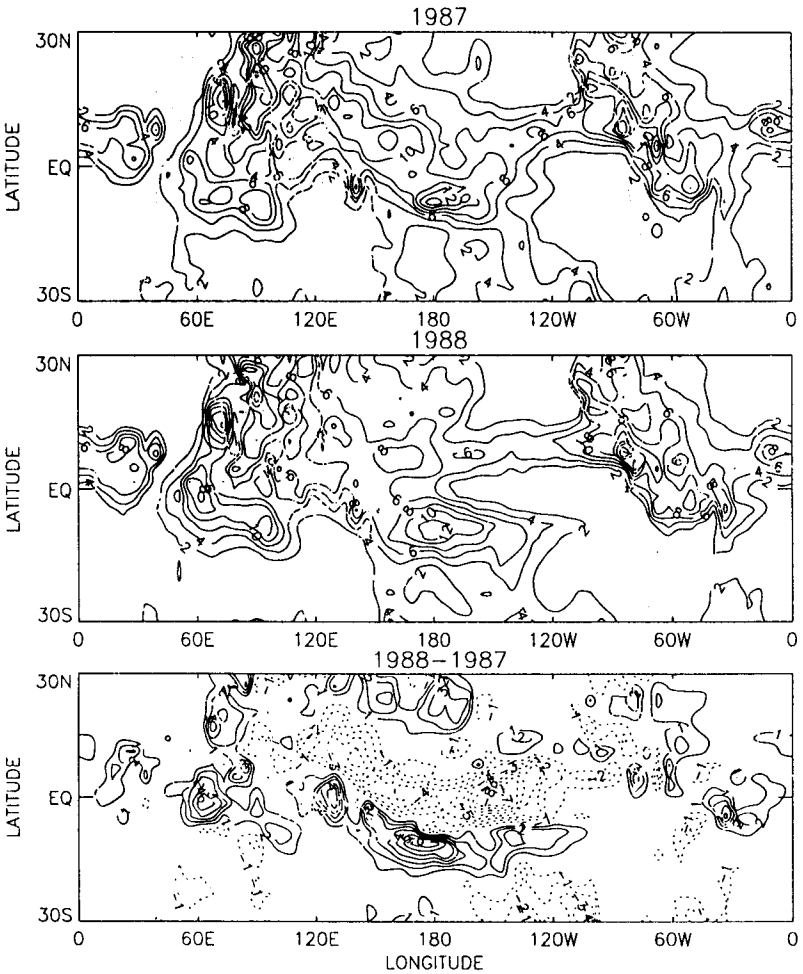

Fig. 9. Same as Figure 8 except for observations.

of equator from 130°E to 160°W, in both observations and simulations (Figs. 8c and 9c), indicate the north-eastward shift of SPCZ during the El Niño year 1987 compared to the La Niña year 1988. Gadgil and Raju (1995) reported that the year to year variability of Indian monsoon rainfall is mostly located over MCZ and west coast of Peninsular India. Even though the simulated rainfall differences between 1988 and 1987 are positive over western Ghats and over MCZ, the amplitudes are too small compared to the observations. In both observations and simulations show an increase in precipitation during 1988 over western part of tropical Indian Ocean and central Africa compared to 1987. However, the model has failed to simulate the observed variability of rainfall over south-west of North America.

4. Results of Experiments 2, 3 and 4

The simulated JJA mean 200mb velocity potential fields during 1988 for the three additional experiments E2, E3 and E4 are shown in Figures 10a, 12a and 14 respectively. The Figures 10b, 12b and 14b are the differences of velocity potential (1988 minus 1987) for E2, E3 and E4 respectively. Krishnamurti (1971) demonstrated that the upper tropospheric planetary scale velocity potential field can be used to estimate the strength of the monsoonal north-south and

east-west circulations. Although the gross features of velocity potential in E1, E2, E3 and E4 are similar, a closer look reveals the differences in the simulations of this field in these four experiments. It can be seen that the divergent inflow center over western hemisphere and the divergent outflow center over eastern hemisphere in E1 shifted eastwards in E3 and E4 for both the years 1987 and 1988 (Figs. 2a, 2c, 12a, 12b, 14a and 14b). The seasonal mean divergent flow over Peninsular India, Arabian sea and Indian Ocean region is weaker in E3 and E4 compared to E1 during both the years 1987 and 1988. In E2, the divergent inflow over Peninsular India is weaker than in E1 during 1987, but during 1988, the simulations of this field in both E1 and E2 are almost similar (Figs. 10a and 10b). Consistent changes can be seen in the simulations of 200 mb TEJ for both the years 1987 and 1988 (Figs. 4a, 4c, 13a, 13b, 15a and 15b). The strength of 200 mb TEJ in E3 and E4 is weaker than that in E1 during 1987 and 1988.

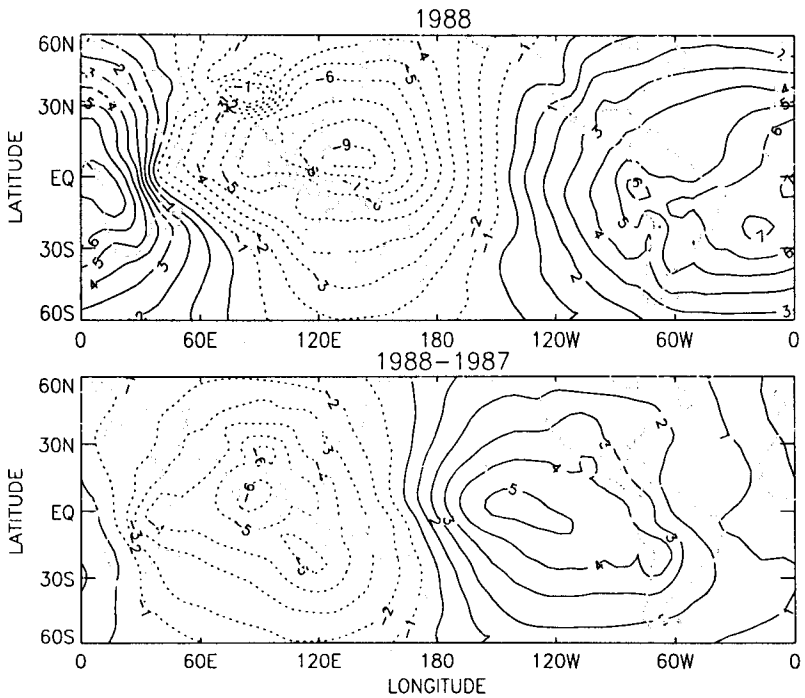

Fig. 10. Modeled(E2) JJA Velocity potential for 1988 (10a) and 1988 minus 1987 (10b) respectively. Contour interval is $1\times10^{6}m^{2}s^{-1}$. Broken lines indicate negative values.

The positive center of the velocity potential differences (1988 minus 1987) is well positioned in E1 (Fig. 2c) like in observations, while in E3 and E4 (Figs. 12b and 14b), it has an eastward displacement. The negative differences of velocity potential between 1988 and 1987 are small over east of Africa, Arabian sea and Indian Ocean in E3 and E4 compared to E1. However, the negative center of velocity potential differences in E2 is stronger than that in E1. The 200 mb wind differences (1988 minus 1987) in E3 show westerlies over north Arabian sea (Fig. 13b), while easterlies are seen in all other model experiments and observations. In all the experiments, the 200 mb wind differences (1988 minus 1987) over 15°N to 15°S and 0° to 120°E are easterlies

like in observations. In E3, the westerly wind differences over 7°S to 6°N are extended to west coast of South America, while in E2 they are extended up to 125°W and there are easterly wind differences over the west coast of South America like in observations.

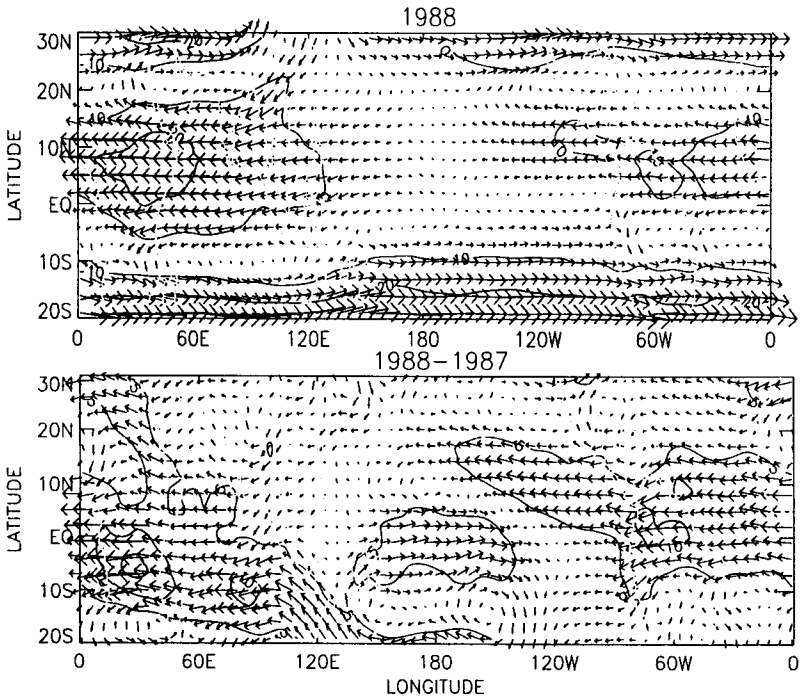

Fig. 11. Modeled(E2) JJA wind for 1988 (11a) and 1988 minus 1987 (11b) respectively. Contours of wind speed are overplotted with contour interval 10 ms^{-1} for 1988 and 5 ms^{-1} for 1988 minus 1987.

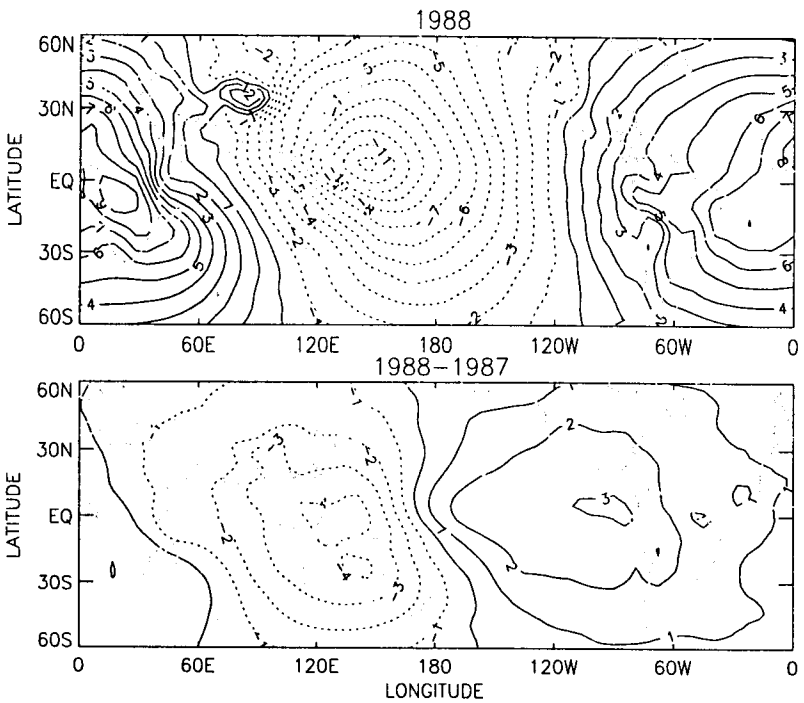

Fig. 12. Modeled(E3) JJA Velocity potential for 1988 (12a) and 1988 minus 1987 (12b). Contour interval is $1\times10^{6}m^{2}s^{-1}$. Broken lines indicate negative values.

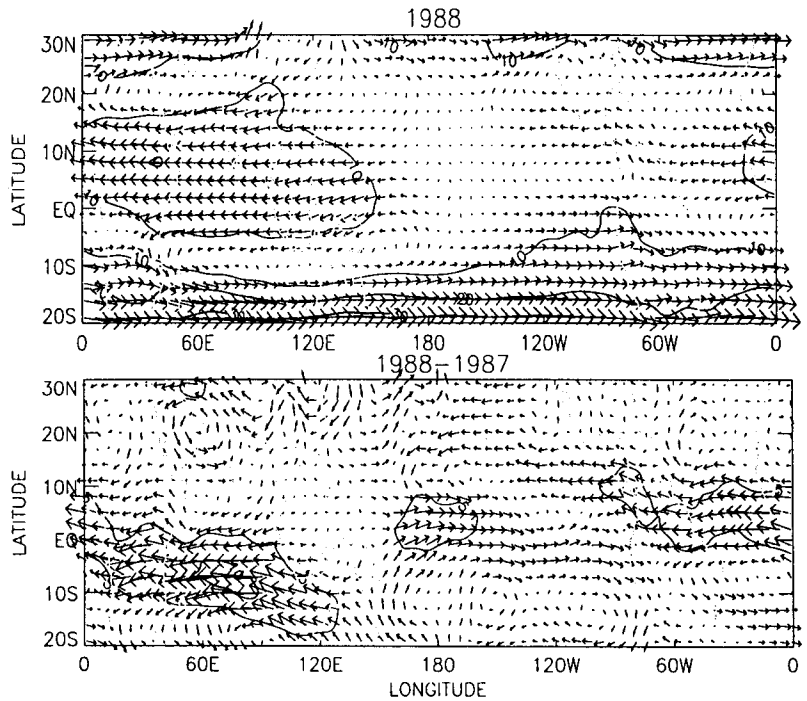

Fig. 13. Modeled(E3) JJA wind for 1988 (13a) and 1988 minus 1988 (13b) respectively. Contours of wind speed are overplotted with contours interval 10 ms^{-1} for 1988 and 5 ms^{-1} for 1988 minus 1987.

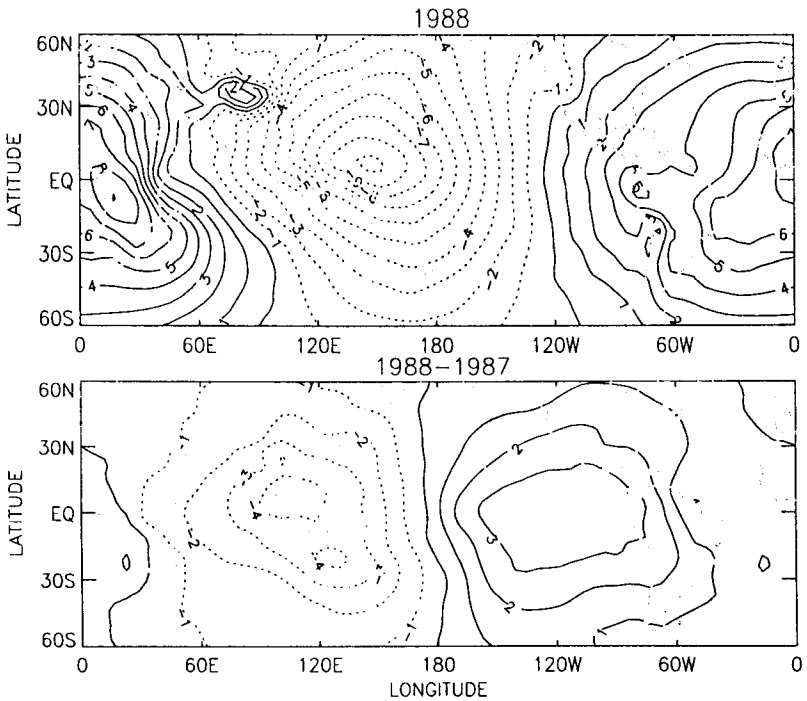

Fig. 14. Modeled(E4) JJA Velocity potential for 1988 (14a) and 1988 minus 1987 (14b) respectively. Contour interval is $1\times10^{6}m^{2}s^{-1}$. Broken lines indicate negative values.

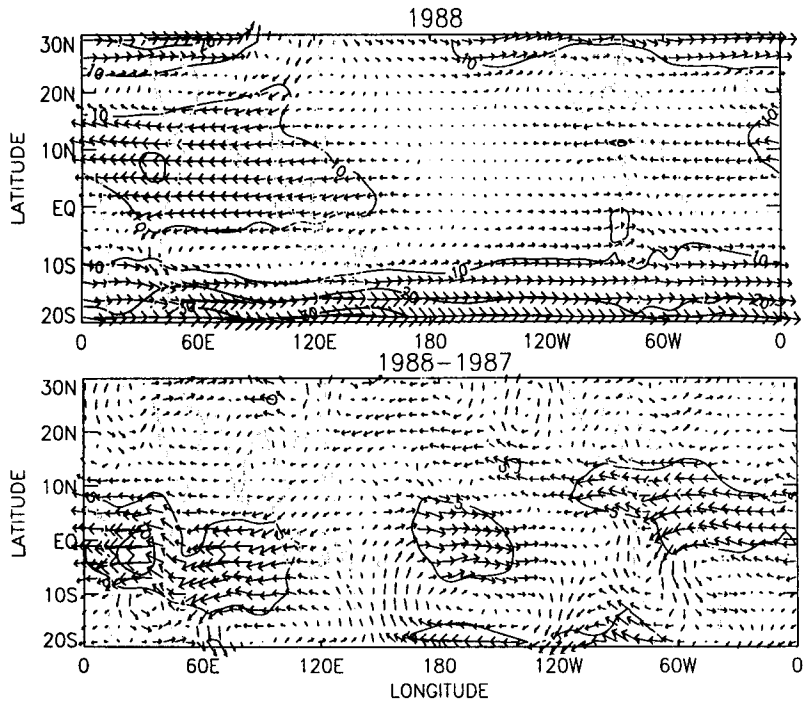

Fig. 15. Modeled(E4) JJA wind for 1988 (15a) and 1988 minus 1988 (15b) respectively. Contours of wind speed are overplotted with contour interval 10 ms^{-1} for 1988 and 5 ms^{-1} for 1988 minus 1987.

5. Discussions and conclusions

In this study, a number of SST forcing experiments were carried out with an AGCM to understand the role of interannually varying SSTs in simulating the broad features of the changes in the observed circulation patterns during 1987 and 1988. The AGCM has been integrated for eight months starting from January 1^{st} with real time monthly mean SSTs of 1987 and 1988. It has been found that, irrespective of its low resolution, AGCM is quite successful in simulating the large-scale features of Asian summer monsoon and its interannual variability. This includes the dipole structure of upper level velocity potential, weakening and eastward migration of divergence and convergence center during 1987 compared to 1987 and decreasing the strength of TEJ during El Niño year 1987. Earlier observational studies reported the weakening of TEJ during warm events (Kanamitsu and Krishnamurti, 1978 and Arkin, 1982). In our simulations, the weakening of TEJ during 1987 compared to 1988 is consistent with the changes in velocity potential during these years. The study of Chen and Loon (1987) demonstrated that the weakening and the eastward shift of divergent circulations aloft during the warm event will weaken the low-level monsoon circulations over Indian Ocean, which will eventually weaken the Tibetan high and upper level divergent circulations by reducing the low-level moisture supply into the subcontinent, cumulus convection and rainfall. Since the energy for maintenance of TEJ is attributed to the balance between the generation of kinetic energy and divergent kinetic energy flux, changes in the monsoon circulations and changes in the tropical divergent circulations during the warm event will reduce the two energetic processes and hence reduce the strength of TEJ (Chen and Loon, 1987).

The distributions of the simulated precipitation field during both the years 1987 and 1988 show some of the observed features like heavy rainfall over foothills of Himalayas, ITCZ over Indian Ocean and 10°N of Africa. The rainfall maxima over west coast of India and MCZ are too weak compared to observations. The poor simulations of rainfall maximum over western Ghats may be related to the coarse resolution of the model and as a result of poor representation of orography over that region. The studies of Fennessy *et al.* (1994), Roy Abraham *et al.* (1996) showed that the correct representation of orography is crucial for the reasonable simulation of Indian summer monsoon. The excessive rainfall over Himalayan region may be at the expense of MCZ since the two rain belt zones are too close together. Thus, an overestimation of orographically forced rainfall over Himalaya may result the weakening of rainfall over MCZ. In the AMIP I integrations, many AGCMs show this deficiency (WMO, 1992).

The simulation of Indian summer monsoon rainfall is a challenging problem and the difficulty is partly due to the special nature of tropical intra-seasonal oscillation (TIO) over the monsoon region. There is an oscillation between two modes of ITCZ with primary mode over the heated subcontinent and the secondary mode over warm Indian Ocean (Sikka and Gadgil, 1980). Since the active and break spells of monsoon rainfall associated with TIO are related to land-surface hydrological processes (Webster, 1983; Goswami and Shukla, 1984; Srinivasan *et al.*, 1993), the surface hydrological processes may be important for the correct simulation of Indian summer monsoon rainfall. In the present simulations, we have not included an interactive hydrology scheme in our model and this may be one of the reasons for the poor simulation of rainfall in our model. A recent study by Laval *et al.* (1996) suggested that although the monsoon characteristics are predominantly associated with SST, it is necessary to represent properly the land surface exchanges to simulate wet and dry monsoon in a realistic way.

It is also possible that the monsoon rainfall may be sensitive to the initial conditions (Palmer *et al.*, 1992). In present work, we have not made any attempt to study the sensitivity of simulated rainfall to initial conditions. Our interest in this study was mainly to understand the role of SSTA alone in simulating the observed variability of large-scale circulations during 1987 and 1988. A more recent study of Dixit *et al.* (1997) pointed out that the active and break phases of TIO can be considered as two equilibrium states of the system and the transition from one phase to another phase occurs in a chaotic way. The chaotic phase transition is largely unpredictable and hence the Indian monsoon may have large unpredictable components.

The modeled precipitation difference (1988 minus 1987) field captured the local effect of SSTA reasonably well. Negative precipitation differences appear from 140°E to west of America where SSTA change its sign associated with the warm and cold phases of ENSO. Other simulated features include the positive precipitation differences between 1988 and 1987 over north of Africa from equator to 15°N and the north-eastward shift of SPCZ associated with El Niño. Rasmusson and Carpenter (1983) showed that the drought years over India are often related to the positive SSTA over equatorial eastern Pacific. In our simulation, AGCM did capture the positive precipitation differences (1988 minus 1987) over Indian subcontinent from south of 20°N. However, the model has failed to simulate the observed amplitude of rainfall difference over north India.

The model integrations with regional SSTA show that the tropical eastern Pacific SSTA have dominant role in the broad-scale changes of atmospheric circulation patterns compared to SSTA over other oceanic regions. Here it is important to note that the global SST integration (E1) is closer to the observations in terms of the position and the strength of circulation patterns. The center of divergent outflow over western Pacific is shifted to east in E3 and E4 compared to E1 during both 1987 and 1988. The weakening of TEJ in E3 and E4 compared to E1 during 1987 and 1988 appears to be related to the weakening of divergent flow over Indian Ocean and monsoon region. The weakening of upper level divergent flow may result in the weakening of low level flow and moisture transport into the subcontinent (Cadet and Diehl, 1984; Shukla, 1986)

and as a result, there is decrease of latent heating which will weaken the Tibetan anticyclone and again the upper level divergent flow. These changes in the divergent flow may cause changes in the energy maintenance of TEJ (Chen and Loon, 1987) and hence the strength of TEJ. Again, the simulation of divergent outflow over Indian Ocean and Asian monsoon region in E2 is weaker than in E1 during 1987, and coherent changes in TEJ can be seen with weakening of TEJ in E2 compared to those in E1 during 1987.

These results suggest that, even though Pacific SSTA play a major role in the interannual variability of tropical circulations, the other regional SSTA, like the SSTA over Indian Ocean, also play some role in the correct simulation of the large-scale monsoonal north-south and east-west divergent circulations and stationary eddies like TEJ in terms of correct position and strength. The finding of Zhu and Houghton (1996) supported this idea that the SSTA over south Indian Ocean will strongly influence the low level flow into the monsoon region and hence the intensity of monsoon. The observational study of Cadet and Diehl (1984), Meehl (1987) also demonstrated the significant role of south Indian Ocean SSTA in changing the strength of monsoon flow. Even though the amplitude of SSTA outside the tropical Pacific is small compared to tropical Pacific, since the mean SST over the regions like Indian Ocean is larger than 28°C, this SSTA can transform into 3-dimensional heating anomaly in the atmosphere and alter the large-scale monsoonal east-west and north-south divergent flow. Changes in the divergent flow may change the stationary eddies and monsoon is a part of stationary eddies (Gill, 1980; Chen and Yen, 1994).

In this study, we have examined the effect of SST forcing on the large-scale flow over tropical and monsoon regions. Our model has captured many observed circulation features of 1987 and 1988. The modeled precipitation shows more local effects of SSTA than remote effects. The integrations with regional SSTA have shown the importance of SSTA outside the tropical Pacific for better simulations of mean JJA circulations during 1987 and 1988

Acknowledgments

The authors wish to thank an anonymous reviewer and the editor whose valuable comments, on a previous version of the manuscript, helped to improve this paper greatly. This work was supported by Indian Space Research Organization (ISRO)-GBP Project.

REFERENCES

Arkin, P. A., 1982. The relationship between interannual variability in the 200 mb tropical wind field and the Southern Oscillation, *Mon. Wea. Rev.*, **107**, 1393-1404.

Barnett, T. P., L. Dumenil, U. Schlese, R. Roeckner, and M. Latif, 1989. The effect of Eurasian snow cover on regional and global climate variations, *J. Atmos. Sci.*, **46**, 661-685.

Biju Thomas, S.V. Kasture and V. Satyan, 2000. Simulation of winter and summer climates with an Atmospheric General Circulation Model (in press), *Mausam*.

Cadet, D. L., and B. C. Diehl, 1984. Interannual variability of surface fields in the Indian ocean during recent decades, *Mon. Wea. Rev.*, **112**, 1921-1935.

Chen, T.-C., and M.-C Loon, 1987. Interannual variations of the tropical easterly jet, *Mon. Wea. Rev.*, **115**, 1739-1759.

Chen, T.-C., and M.-C Yen, 1994. Interannual variations of the monsoon simulated by the NCAR community climate model: Effect of the tropical Pacific SST, *J. Climate*, **7**, 1403-1415.

Dixit, S., T. N. Palmer, and P. J. Webster, 1997. Are Monsoon chaotic? Implications for the predictability of intraseasonal and interannual monsoon variability, Submitted to *J. Climate*

Druyan, L. M., and S. Hastenrath, 1994. Tropical impacts of SST forcing: A case study for 1987 versus 1988, *J. Climate*, **7**, 1316-1323.

Fennessy, M. J., 1993. MONEG related research at COLA: Simulation and prediction of monsoons. Recent results. TOGA/WGNE monsoon numerical experimentation group, New Delhi, India, 12-14 January 1993. WCRP-80, WMO/TD-No. 546.

Fennessy, M. J., J. L. Kinter III, B. Kirtman, L. Marx, S. Nigam, E. Schneider, J. Shukla, D. Straus, A. Vernekar, Y. Xue, and J. Zhou, 1994. The simulated Indian monsoon: A GCM sensitivity study, *J. Climate*, **7**, 33-43.

Frederiksen, C. S., K. Puri, and R. C. Balgovind, 1992. Intraseasonal variation and simulation of Indian summer monsoon. Simulation of interannual and intraseasonal monsoon variability: Report of workshop, National Center for Atmospheric Research, Colorado, USA, 21-24 October 1991, WCRP-68, WMO/TD-No. 470.

Gadgil, S., Asha Guruparasd, D. R. Sikka, and D. K. Paul, 1992. Intraseasonal variation and simulation of Indian summer monsoon. Simulation of interannual and intraseasonal monsoon variability: Report of workshop, National Center for Atmospheric Research, Colorado, USA, 21-24 October 1991, WCRP-68, WMO/TD-No. 470.

Gadgil, S., and A. Raju, 1995. Simulation of the Indian summer monsoon rainfall and its interannual variation in the AMIP runs. Proceedings of the first international AMIP scientific conference, Monterey, California, USA, 15-19 May 1995. WCRP-92, WMO/TD-No. 732.

Gill, A. E., 1980. Some simple solutions for heat-induced tropical circulations, *Q. J. R. Meteorol. Soc.*, **106**, 447-462.

Goswami, B. N., and J. Shukla, 1984. Quasi-periodic oscillations in a symmetric general circulation model, *J. Atmos. Sci.*, **41**, 20 -37.

Ju, J., and J. Slingo, 1995. The Asian summer monsoon and ENSO, *Q. J. R. Meteorol. Soc.*, **121**, 1133-1168.

Kanamitsu, M., and T. N. Krishnamurti, 1978. Northern summer tropical circulations during drought and normal rainfall months, *Mon. Wea. Rev.*, **106**, 331-347.

Krishnamurti, T. N., 1971. Tropical east-west circulations during the northern summer, *J. Atmos. Sci.*, **28**, 1332- 1347.

Krishnamurti, T. N., H. S. Bedi, and M. Subramaniam, 1989. The summer monsoon of 1987, *J. Climate*, **2**, 321- 340.

Krishnamurti, T. N., H. S. Bedi, and M. Subramaniam, 1990. The summer monsoon of 1988, *Meteor. Atmos. Phys.*, **42**, 19-37.

Laval, K., R. Raghava, J. Polcher, R. Sadourny, and M. Forichon, 1996. Simulations of the 1987 and 1988 Indian monsoons using the LMD GCM, *J. Climate*, **9**, 3357-3371.

Legates, D. R., and C. J. Willmott, 1990. Mean seasonal and spatial variability in gauge-corrected global precipitation. *Int. J. of Climatol.*, **10**, 111-128.

Meehl, G. A., 1987. The annual cycle and interannual variability of the tropical Pacific and Indian ocean regions, *Mon. Wea. Rev.*, **115**, 27-50.

Meehl, G. A., 1994. Influence of the land surface in the Asian summer monsoon: External conditions versus internal feedbacks, *J. Climate*, **7**,1033-1049.

Mo, K. C., 1992. Impact of SST anomalies on the skill of seasonal forecasts and northern summer monsoons, *J. Climate*, **5**, 1249-1266.

Palmer, T. N., Brankovic, P. Viterbo, and M. J. Miller, 1992. Modeling interannual variations of summer monsoons, *J. Climate*, **5**, 399-417.

Rasmusson, E. M., and T. H. Carpenter, 1983. The relationship between eastern Pacific sea surface temperature and rainfall over India and Sri Lanka, *Mon. Wea. Rev.*, **111**, 517-528.

Reynolds, R. W., and D. C. Marisco, 1993. An improved real-time global sea surface temperature analysis, *J. Climate*, **6**, 114-119.

Roy Abraham, K., S. K. Dash and U. C. Mohanty, 1996. Simulation of monsoon circulations and cyclones with different types of orography, *Mausam*, **47**, 237-250.

Shukla, J., and D. A. Paolino, 1983. The southern oscillation and long range forecasting of the summer monsoon rainfall over India, *Mon. Wea. Rev.*, **111**, 1830-1837.

Shukla, J., 1986. SST anomalies and blocking, *Advances in Geophysics*, **29**, 443-452.

Shukla, J., and M. Fennessy, 1994. Simulation and predictability of monsoon: Proceedings of the international conference of monsoon variability and prediction. International center for theoretical physics, Trieste, Italy, 9-13 May 1994, WCRP, WMO/TD-No. 619, 567-575.

Sikka, D. R., and S. Gadgil, 1980. On the maximum cloud zone and the ITCZ over Indian longitudes during the southwest monsoon, *Mon. Wea. Rev.*, **108**, 1840-1853.

Srinivasan, J., S. Gadgil and P. J. Webster, 1993. Meridional propagation of large-scale monsoon convective zones, *Meteor. Atmos. Phys.*, **52**, 15-35.

Sud, Y. C., and W. E. Smith, 1985. Influence of local land surface processes on the Indian Monsoon: A numerical study, *J. Climate and Appl. Meteor.*, **24**, 1015-36.

Trenberth, K. E., 1976. Spatial and temporal variations of the southern oscillations, *Q. J. R. Meteorol. Soc.*, **102**, 639-53.

Vernekar, A. D., J. Zhou and J. Shukla, 1995. The effect of Eurasian snow cover on the Indian monsoon, *J. Climate*, **8**, 248-265.

Webster, P. J., 1983. Mechanisms of monsoon low- frequency variability: Surface hydrological effects, *J. Atmos. Sci.*, **40**, 2110-2124.

WMO (World Meteorological Organization), 1992. Simulation of interannual and intraseasonal monsoon variability. Report of workshop, National Center for Atmospheric Research, Boulder, Colorado, U.S.A., 21-24 October 1991. WCRP - 68, WMO/TD - No.470.

Yang, S., 1996. ENSO-Snow-Monsoon associations and seasonal- interannual predictions, *Int. J. Climatol.*, **16**, 125-134.

Zhu, Y. L., and D. D. Houghton, 1996. The impact of Indian ocean SST on the large-scale Asian summer monsoon and the hydrological cycle, *Int. J. of Climatol.*, **16**, 617-632.